pISSN 1229-3008 eISSN 2287-6251
Progress in Superconductivity and Cryogenics
Vol.19, No.2, (2017), pp.9~13 https://doi.org/10.9714/psac.2017.19.2.009

Effects of seed orientation on the growth behavior of single grain REBCO bulk superconductors

Hee-Gyoun Lee*

Korea Polytechnic University, Siheung, Korea

(Received 18 April 2017; revised or reviewed 10 May 2017; accepted 11 May 2017)

Abstract

This study presents a simple method to control the seed orientation which leads to the various growth characteristics of a single grain REBCO (RE: rare-earth elements) bulk superconductors. Seed orientation was varied systematically from c-axis to a-axis with every 30 degree rotation around b-axis. Orientations of a REBCO single grain was successfully controlled by placing the seed with various angles on the prismatic indent prepared on the surface of REBCO powder compacts. Growth pattern was changed from cubic to rectangular when the seed orientation normal to compact surface was varied from c-axis to a-axis. Macroscopic shape change has been explained by the variation of the wetting angle of un-reacted melt depending on the interface energy between $YBa_2Cu_3O_{7-y}$ (Y123) grain and melt. Higher magnetic levitation force was obtained for the specimen prepared using tilted seed with an angle of 30 degree rotation around b-axis.

Keywords: Single grain REBCO, Bulk superconductors, Seed orientation, Facet lines, Shape change

1. INTRODUCTION

High performance single-grain $REBa_2Cu_3O_{7-y}$ (RE123, RE: rare-earth elements) bulk superconductors have been fabricated by a top-seeded melt growth (TSMG) process [1–3]. However, extended heat treatment is needed to grow large single-grain REBCO bulk superconductors because the peritectic growth reaction of REBCO grains is sluggish. In order to shorten the processing period, Kim et al. [4] developed an interior seeding technique that the interior seed has realize two-directional growth into both upward and downward directions that resulted in the reduced processing time together with the improvement of material quality. On the other hand, multi-seeding technique [5, 6] has been also used in order to fasten the processing time. Multi-seeding technique needs to control seed orientation in order to avoid the formation of high angle grain boundaries that are formed by the impingement of the grains grown from different seeds [7]. In TSMG processes, seeds are placed on the outer surfaces of the powder compacts; in the center [1–3, 6, 8, 9], of the top surfaces or on the bottom [10], on the corner [11]. All these seeded melt growth technique, seed placed as that c-axis of seed is normal to the surface of the powder compact

Jung et al. [12] have reported that the magnetic properties of melt-grown REBCO single grain vary with the crystal orientation of a YBCO grain. The c-axis oriented YBCO grain showed the highest magnetic trap field and levitation force. The orientation dependence of the magnetic properties was originated from the anisotropic grain growth behavior and the critical current density of REBCO crystal. Kim el al.,[4] also suggested that a-c growth sector (c-axis gown region) is inferior to a-b growth sector (a- or b-axis grown region) due to fast growth rate in c-axis. Therefore, the observations of seed orientation on the growth behavior of REBCO grains by TSMG may give fundamental idea how the growth pattern and growth behavior are varied with seed orientation. The size of a seed crystal is so small that it is not easy to cut the seed crystal with a desired orientation at will. Therefore, it may be helpful if the seed orientation is controlled systematically with ease.

In this article, a simple method in controlling the seed orientation is introduced in order to fabricate the large REBCO grains with various orientations. The relationships of the growth pattern, shape change and the magnetic properties of REBCO grains with seed orientation are discussed in terms of the observed grain growth behaviors and the measured magnetic properties.

2. EXPERIMENTALS

$Y_{1.5}Ba_2Cu_3O_{7-y}$ (hereafter Y1.5) powder was used as a raw material in this study. Y1.5 powder was made by mixing 1 mole Y123 (Solvay Germany, 99.9 % purity, 2–3 μm in size) with 0.25 mole Y_2O_3 (BM-CHEM HI-TECH Co., Ltd, China, 99.99 % purity, 0.12–3 μm in size) powder. 1 wt. % CeO_2 powder was added to the Y1.5 powder to refine Y_2BaCuO_5 (Y211). An appropriate amount of Y1.5 powder was put into a steel mold with a diameter (d) of 20 mm. In order to perform TSMG, Sm123 seeds were used.

* Corresponding author: hglee@kpu.ac.kr

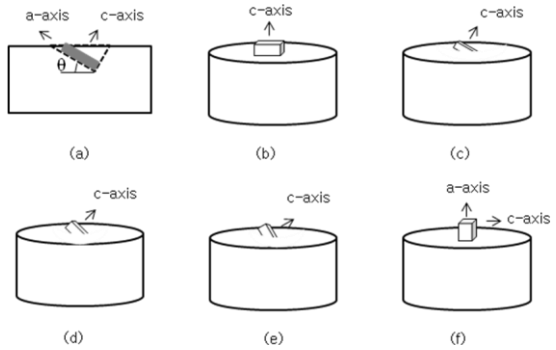

Fig. 1. Schematic drawings showing the seeding method. (a) Cross sectional view showing how the rotation angle around b-axis is controlled. (b)-(f) shows the seeds with the rotation angle from 0° to 90° with an interval of 30°.

Fig. 1(a) shows a schematic drawing how the seed orientation was controlled. The surface grooves, which have the right-angled triangular prism cross section, were provided at the center of powder compact with the variation of ramp angle(denoted as θ in Fig. 1(a)) with 30, 45 and 60 degree and placed the seed on the powder compact surface as shown in Fig. 1(a). Surface grooves were prepared by placing right-angle triangular prism-shaped 3 mm-thick rubber inserts with different angles. The Y1.5 powder with the insert was pressed into the pellet. After pressing, the powder compact was taken out of the pressing die and the insert was removed from the top of the powder compact. Platelet c-axis Sm123 seed was placed on tapered ramp with various angles of 30, 45 and 60 degree. Figs. 1(b)-(e) depict the schematic drawings of the seeds with different orientations. The heat treatment procedure for TSMG was similar to those reported in the literature [13]. The cooling rate controlled with 0.25℃h^{-1} at the temperature regime for the growth of Y123 grains. After the TSMG heat treatment, Y1.5 samples were heated to 500℃ at a rate of 200℃h^{-1} in flowing oxygen for oxygenation, held at this temperature for 50 h, cooled to 400–500℃ at a rate of 100℃h^{-1}, held at this temperature for 200-300 h, and then cooled to room temperature at a rate of 200℃h^{-1}.

Magnetic levitation forces and trapped magnetic fields at 77 K were measured for the top surface of the field-cooled (FC) or zero field-cooled (ZFC) samples. Force-distance curves were obtained by measuring the force exerting on the magnet when the permanent magnet was approached to the superconductors which were cooled to 77 K under no external magnetic field (zero field cooling, ZFC). A Nd-B-Fe magnet with a surface field of 520 mT was used for the FC experiment. The trapped magnetic fields of the top surfaces of the FC samples were measured using a Hall probe. Force–distance curve (F–d) at 77 K was obtained for the ZFC samples. For the levitation force measurement, Nd-B-Fe permanent magnets with d=30 mm were used. Maximum magnetic levitation force at 77 K was defined as the force when the permanent magnet is distanced 0.1 mm from the superconductor surface.

3. RESULTS AND DISCUSSSION

Fig. 2 shows the photos of the top surfaces of the samples after melt growth (MG) heat treatment. The diameter of the sample was reduced after the MG heat treatment. It is seen that all the specimens have four facet lines irrespective of seed orientation ($0° < \theta < 90°$) but the angles between the X-shaped facet lines varies with the seed orientation. The crystallographic planes of seeds with different rotation angles (theta, θ) are presented in Table I. The angle between the facet lines decreases with the rotation angle up to $\theta = 60°$ and bounds back to 90° at $\theta = 90°$.

In order to observe the X-shaped facet more clearly, top surface of the specimens was ground out and the growth patterns were photographed as in Fig. 3. Pattern shapes are not clear yet to measure the angle between facet lines and therefore the facet lines are drawn schematically in Fig. 4. It is observed that the angle between the facet lines tends to decrease with the rotation angle up to $\theta = 60°$ but the actual angle between the facet lines far from the calculated values in Table I. The calculated angles in Table I were obtained based on the assumption that the growth rates of a Y123 grain in a-axis, b-axis and c-axis are identical. However, the growth rate of Y123 grain may vary with the crystallographic orientation. Nakamura et al. [14] reported

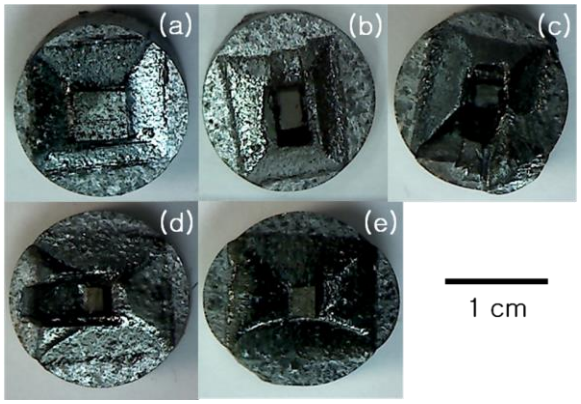

Fig. 2. Photos of the top surface of the TSMG specimens. Rotation angles of seed are (a) 0°, (b) 30°, (c) 45°, (d) 60° and (e) 90°.

TABLE I
THE CRYSTALLOGRAPHIC PLANES OF SEEDS WITH RESPECTIVE TO THE SPECIMEN TOP SURFACE WITH DIFFERENT ROTATION ANGLES (θ IN FIG.1(A)) AROUND B-AXIS.

Rotation angles	0°	30°	45°	60°	90°
Crystallographic plane	(001)	(102)	(101)	(201)	(100)
Crystallographic direction of facet lines	<110>	<221>	<111>	<112>	<011>
Angle between facet lines	90°	83.6°	70.5°	48°	90°

*The calculation of the angle between the facet lines was performed based on the assumption that the lattice parameters of a-axis, b-axis, and the 1/3 of the lattice parameter of c-axis have the same value like a cubic structure and the growth rates of Y123 crystal are same regardless of crystallographic directions.

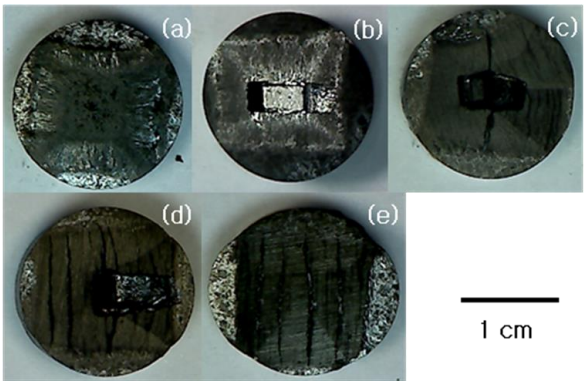

Fig. 3. Photos showing the facet line patterns formed on the top surface of the TSMG specimens after surface grinding. Rotation angles of seed are (a) 0°, (b) 30°, (c) 45°, (d) 60° and (e) 90°.

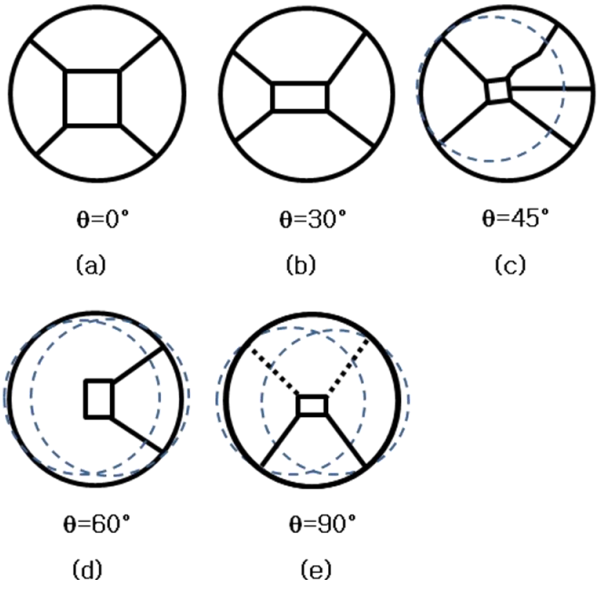

Fig. 4. Schematic drawings of the facet line patterns and the dotted circles showing the radius of curvature of the un-reacted melts solidified after melt process. Rotation angles of seed are (a) 0°, (b) 30°, (c) 45°, (d) 60° and (e) 90°.

that the growth rate of Y123 grain varies with the crystallographic orientation as well as the undercooling for grain growth and the amount of Y211 particles in the front of the growing grains. It means that the X-shaped facet lines pattern are formed through much complex procedure. Therefore, further works are needed in order to validate the relationship between the angles of X-shaped facet lines and the seed orientation.

In Fig. 3, it is also seen that the macroscopic cracks were formed for the specimens with θ = 45°, 60°, and 90°. For the specimen with θ = 45°, cracks appears predominantly at the right half of the grown grain while cracks are covers whole grain in the specimens with θ = 60° and 90°. Kim et al. [4] has developed an interior seeding technique and successfully showed that the inverse octahedral growth pattern is formed for the upper part of the specimen when the seed was placed in the center of the specimen. It means that an asymmetric microstructure develops if a seed crystal is tilted with respect to the specimen surface. The partial development of cracks in Fig. 3(c) is possibly explained by the assumptions that the left half of the grown grain represents the a-axis growing sector and the right half of the grown grain with macroscopic cracks is the c-axis grown sector.

Additionally, Fig. 4 shows that the sample shapes for θ = 60° and 90° vary from circular cross section to an oval cross section during a melt process. The photos of the polished specimens show that the specimens are divided into two regions of the grown grain and the un-reacted solidified melts.

Figs. 4(c)-(e) show the schematic drawings showing that the macroscopic shape changes can be described by two circles with different diameters. The specimens with θ = 0° and 30° have a circular cross section with a diameter of radius of 1.7 mm but the cross sections of the specimens with θ = 60°, and 90° are consisted of two areas which can be characterized using the circles with different diameters; central parts are consisted of the Y123 grain with a diameter of 1.69~1.7 mm and two ends are consisted of the solidified melts with a diameter of 1.4~1.5 mm. It is noticeable that two ends having small radius of curvature are the directions parallel to c-axis (i.e., normal to (001) plane). It is known that the (001) crystallographic plane of Y123 has a lowest surface energy and therefore the interfacial energy between the (001) plane of Y123 and melt is also minimum. Low interfacial energy resulted in a large wetting angle of the melt on the (001) plane of Y123 compared to those on the other crystallographic planes. At the later stage of the growth of Y123 grain, un-reacted melt is remained on the specimen surface and walls. Depending on the crystallographic orientations, the wetting angle of the remnant melt varies and the specimen wall normal to c-axis growth front has a small radius of curvature due to its low interfacial energy. Diko and Goretta [15] reported that a distortion from circular cross-section is attributed to liquid transport from a slower growth front in a-axis direction to a faster growth front in a c-axis direction at the edge between the a-growth and c-growth fronts. Iida et al., [16] has shown that the macroscopic shape change of specimen occurs for the $BaZrO_3$ particle doped YBCO specimen prepared by TSMG method. The addition of $BaZrO_3$ increased the amount of 211 particles in the melts during the growth of Y123 single grain and led to a prominent shape changes. It seems that the $BaZrO_3$ addition may change the melt chemistry and thereby the interfacial energy between Y123 grain and the melt. Namburi et al. [17] also has reported the shape change in the YBCO specimen prepared by TSIG (Top-seeded Infiltration Growth) method when the pre-sintering temperature of Y211 pellets was lower than 1050 ℃. Therefore, it is thought that the distortion of the melt

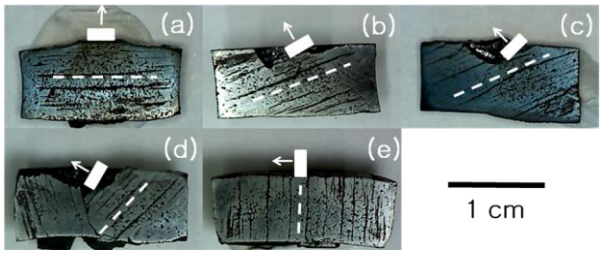

Fig. 5. Photos showing the cracks in the cross sections of the TSMG specimens. Rotation angles of seed are (a) 0°, (b) 30°, (c) 45°, (d) 60° and (e) 90°. White rectangles denote the seeds and arrows represents the <001> directions of seeds. Dotted lines indicate the crack lines on (001) planes.

processed specimens might be closely related to the melt chemistry during the synthesis of REBCO superconductors. From the observations of Figs. 2, 3 and 4, the shape changes from the seed tilting (or rotation) were able to explain in terms of the interfacial energy differences in various crystallographic planes without the assumption of liquid transport suggested by Diko and Goretta[15].

Fig. 5 shows the cracks in the cross sections of the TSMG specimens. Rotation angles of seed are (a) 0°, (b) 30°, (c) 45°, (d) 60° and (e) 90°. White rectangles denote the seeds that were placed on cold compact before melt process. Dotted lines indicate the crack lines on (001) planes which have been developed during oxygenation heat treatment. It can be seen that the crack lines are not parallel to the (001) planes of seeds. The angles between the crack lines and the compact surface were measured as 0°, 21°, 24°, 47°, and 90° for the specimens with the rotation angle of seeds of 0°, 30°, 45°, 60° and 90°, respectively. The specimens with θ=0° and 90°, the angles between the crack lines and the specimen surface coincide with the angles formed between (001) plane and the specimen surface. The deviations of the crack orientations from the seed orientations were 9°, 21° and 13° for the specimens with the rotation angle of seeds of 30°, 45°and 60°, respectively. The deviations from the seed orientation and the crack orientations in (001) plane may attribute to the dimensional changes of the compacts during the melt process at high temperature where the specimens is present as a mixture of melt and second phase particles. It has been known that there are dimensional changes of the compacts during the melt process in both of lateral and vertical directions through the melt processing of REBCO superconductors. These dimensional changes are dependent on the melt chemistry as well as the processing temperature, the amount of Y211 particles and so on. In this study, the melt processing has been performed by using Y1.5 compacts which have large dimensional change of 12.2% compared with relatively small change of 2% for Y211 compact [18]. In order to make a qualitative analysis of the seed rotation during the melt process, more elaborated experimental design is needed.

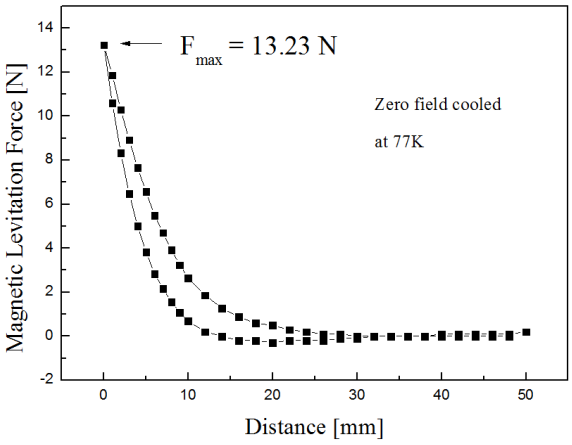

Fig. 6. A typical example of a F-d curve of a melt grown YBCO superconductor.

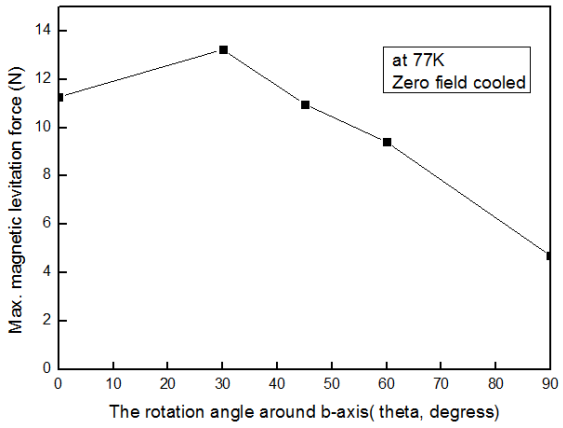

Fig. 7. Variation of the maximum magnetic levitation forces at 77K of the TSMG specimens with various angles of seed rotation around b-axis. Rotation angles of seed are (a) 0°, (b) 30°, (c) 45°, (d) 60° and (e) 90°.

Fig. 6 shows a typical example of F-d hysteresis curve at 77 K of the ZFC specimen. The repulsive magnetic force (F) induced by the Meissner effect of the superconductor is negligible until the distance, d, becomes 10 mm. We measured F-d curves for all specimens to understand the maximum levitation force at d=1 mm.

Fig. 7 shows the variation of the maximum magnetic levitation forces at 77 K of the ZFC specimens, which were prepared by TSMG using the seeds with different orientation. It is seen that the levitation force is 11.3 N for the specimen prepared by using the seed of θ = 0° (c-axis is normal to sample surface), reaches to a maximum force of 13.2 N for is for the sample of θ = 30°, and then gradually decreases down to 4.7 N as the rotation angle of seed around b-axis increases to 90° (a-axis is normal to sample surface). Jung et al. [10] reported that the magnetic levitation is maximum for the specimen with θ = 0° and the levitation forces are similar for the specimens where each a-axis, b-axis and <110>-axis is normal to the pellet surface.

They explained the orientation dependence of levitation force is mainly due to the difference of critical current density (J_c) with crystallographic planes. As seen in Fig. 3, the polished surface showed severe macroscopic cracks for the specimens with $\theta = 45^\circ$, 60°, and 90°. The macroscopic crack is one of the detrimental defects which result in the decrease of J_c and followed drop of magnetic levitation force. The generation and propagation of cracks is closely related to the presence of second phase particle of Y211 in Y123 superconductor matrix. The areas with cracks also contain less second phase particles, which is possibly beneficial for the flux pinning, compared to those without cracks.

In order to explain the high levitation force of the specimen with $\theta = 30^\circ$, it is needed to quantify the effects of several variables of the microstructure, orientation, and the size and amount of 211 particles on the magnetic and electrical properties of TSMG specimens. As seen in Fig.5, all the specimens show severe cracks with a difficulty to compare which one is better. Simply comparing two specimens with $\theta = 0^\circ$ and 30°, it is seen that the c-axis growth sector is more prominent in the specimen with $\theta = 0^\circ$ than in the specimen with $\theta = 30^\circ$. The increase of a-axis growth sector in the specimen with $\theta = 30^\circ$ might be related to the slight increase of magnetic levitation force relative to that of the specimen with $\theta = 0^\circ$. However, it is still lack of detailed data to determine the separated effects from each variable of the microstructure, orientation, and the size and amount of Y211 particles on the magnetic and electrical properties of TSMG specimens.

4. CONCLUSIONS

Single grain REBCO (RE: rare-earth elements) bulk superconductors have been synthesized by controlling the seed orientation with ease. Seed orientation was varied systematically from c-axis to a-axis with every 30 degree rotation around b-axis. Orientation control was achieved by putting the seed with various angles on the prismatic indent prepared on the surface of REBCO powder compacts. Growth pattern was changed from cubic to rectangular when the seed axis normal to compact surface was varied from c-axis to a-axis by rotating around b-axis. Macroscopic shape change has been explained by the changes of wetting behavior of un-reacted melt because the wetting angle decreases with the decrease of the interface energy between Y123 grains and melt during melt processing. Highest magnetic levitation force was shown for the specimen prepared using tilted seed with an angle of 30 degree rotation around b-axis.

ACKNOWLEDGEMENTS

Author is grateful to Park S. D. and Park J. E. for their helps for the sample preparation and the magnetic measurements.

REFERENCES

[1] M. Morita, S. Takebayashi, M. Tanaka, K. Kimura, K. Miyamoto and K. Sawano, "Quench and melt growth (QMG) process for large bulk superconductor fabrication," *Adv. Supercond*., vol. 3, pp. 733-736, 1991.

[2] S. Meslin and J. G. Noudem, "Infiltration and top seeded grown mono-domain $YBa_2Cu_3O_{7-x}$ bulk superconductor," *Supercond. Sci. Technol*., vol. 17, pp. 1324-1328, 2004.

[3] C. Varanasi, P. J. McGinn, V. Pavate and E. P. Kvam, "논문제목," *J. Mater. Res*., vol. 10 , pp. 2251-2256, 1995

[4] C. -J. Kim, S. -D. Park, H . -W. Park and B. -H. Jun, "Interior seeding for the fabrication of single-grain REBCO bulk superconductors," *Supercond. Sci. Technol*., vol. 29, pp. 034003-034009, 2016.

[5] P. Schaetzle, G. Krabbes, G. Stover, G. Fuchs and D. Schlafer, "Multi-seeded melt crystallization of YBCO bulk material for cryogenic applications," *Supercond. Sci. Technol*., vol. 12, pp. 69–76, 1999.

[6] Y. A. Jee, C. -J. Kim, T. -H. Sung, G. -W. Hong, "Top-seeded melt growth of Y-Ba-Cu-O superconductor with multiseeding," *Supercond. Sci. Technol*., vol. 13, pp. 195-201, 2000.

[7] T. D. Withnell, N. H. Babu, K. Iida, Y. Shi, D. A. Cardwell, S. Haindl, F. Hengstberger and H. W. Weber, "The effect of seed orientation and separation on the field trapping properties of multi-seeded, melt processed Y–Ba–Cu–O," *Physica C*, vol. 445–448, pp. 382–386, 2006

[8] M. Sawamura, M. Morita and H. Hirano, "A new method for multiseeding RE–Ba–Cu–O superconductor," *Supercond. Sci. Technol*., vol. 17, pp. S418-421, 2004.

[9] L. Cheng, L. S. Guo, Y. S. Wu, X. Yao and D. A. Cardwell, "Multi-seeded growth of melt processed Gd–Ba–Cu–O bulk superconductors using different arrangements of thin film seeds," *J. Cryst. Growth*, vol. 366, pp. 1-7, 2013.

[10] C. -J. Kim, Y. A. Jee, S. C. Kwon, T. H. Sung and G. W. Hong, "Control of YBCO growth at the compact/substrate interface by bottom seeding and Yb_2O_3 coating in seeded melt-growth processed YBCO oxides using a MgO substrate," *Physica C*, vol. 315, pp. 263-270, 1999.

[11] C. -J Kim, S. -A. Jung, H. -W. Park, B. -H. Jun and S. -D. Park, "Top surface morphologies of melt growth processed bulk superconductors with corner or edge seeding," *Physica C*, vol. 495, pp. 225-228, 2013.

[12] Y. Jung, S. J. Go, H. T. Joo, Y. J. Lee, S. -D. Park, B. -H. Jun and C. -J. Kim, "Orientation and thickness dependence of the magnetic levitation force and trapped magnetic field of single grain $Y_{1.5}Ba_2Cu_3O_{7-y}$ bulk superconductors," *Prog. Supercond. Cryog.*, vol. 19, pp. 30-34, 2017.

[13] C. -J. Kim, Y. A. Jee, G. -W. Hong, T. -H. Sung, Y. -H. Han, S. -C. Han, S. -J. Kim, W. Bieger and G. Fuchs, "Effects of the seed dimension on the top surface growth mode and the magnetic properties of top-seeded melt growth processed YBCO superconductors," *Physica C*, vol. 331 , pp. 274-284, 2000.

[14] Y. Nakamura, A. Endo and Y. J. Shiohara, "The relation between the undercooling and the growth rate of $YBa_2Cu_3O_{6+x}$ superconductive oxide," *Mater. Res*., vol. 11, pp. 1094-1100, 1996.

[15] P. Diko and K. C. Goretta, "Macroscopic shape change of melt-processed $YBa_2Cu_3O_x/Y_2BaCuO_5$ bulk superconductors," *Physica C*, vol. 297 , pp. 211-215, 1998.

[16] K. Iida, N. H. Babu, Y-H. Shi and D. A. Cardwell, "The effect of the addition of zirconium-containing compounds on the microstructure and superconducting properties of mono-domain Y–Ba–Cu–O bulk superconductors," *Supercond. Sci. Technol.*, vol. 18, pp. 704-709, 2005.

[17] D. K. Namburi, Y. Shi, K. G. Palmer, A. R. Dennis, J. H. Durrell and D. A. Cardwell, "An improved top seeded infiltration growth method for the fabrication of Y–Ba–Cu–O bulk superconductors," *J. Europ. Ceram. Soc.*, vol. 36, pp. 615-624, 2016.

[18] J. H. Lee, S. D. Park, B. H. Jun, J. S. Lee, S. C. Han, Y. H. Han and C. J. Kim, "A buffer bridge process for growing multiple $YBa_2Cu_3O_{7-y}$ grains from one top seed," *Supercond. Sci. Technol*., vol. 24, pp. 055019-055025, 2011.